HHS Public Access

Author manuscript

J Biomol Struct Dyn. Author manuscript; available in PMC 2023 October 01.

Published in final edited form as:

J Biomol Struct Dyn. 2022 October ; 40(16): 7367–7380. doi:10.1080/07391102.2021.1901144.

Antiretroviral drug activity and potential for pre-exposure prophylaxis against COVID-19 and HIV infection

Dennis C. Copertino Jr[1], **Bruno C. Casado Lima**[1], **Rodrigo R. R. Duarte**[1], **Timothy R. Powell**[1], **Christopher E. Ormsby**[2], **Timothy Wilkin**[1], **Roy M. Gulick**[1], **Miguel de Mulder Rougvie**[1,#], **Douglas F. Nixon**[1,#,*]

[1]Division of Infectious Diseases, Weill Cornell Medicine, Cornell University, New York, NY, USA.

[2]Center for Research in Infectious Diseases (CIENI), National Institute of Respiratory Diseases (INER), Mexico City, Mexico

Abstract

COVID-19 is the disease caused by SARS-CoV-2 which has led to 2,477,000 deaths worldwide, a number which is rapidly increasing. Urgent studies to identify new antiviral drugs, repurpose existing drugs, or identify drugs that can target the overactive immune response are ongoing. Antiretroviral drugs (ARVs) have been tested in past human coronavirus infections, and also against SARS-CoV-2, but a trial of lopinavir and ritonavir failed to show any clinical benefit in COVID-19. However, there is limited data as to the course of COVID-19 in people living with HIV, with some studies showing a decreased mortality for those taking certain ARV regimens. We hypothesized that ARVs other than lopinavir and ritonavir might be responsible for some protection against the progression of COVID-19. Here, we used chemoinformatic analyses to predict which ARVs would bind and potentially inhibit the SARS-CoV-2 main protease (Mpro) or RNA-dependent-RNA-polymerase (RdRp) enzymes *in silico*. The drugs predicted to bind the SARS-CoV-2 Mpro included the protease inhibitors atazanavir and indinavir. The ARVs predicted to bind the catalytic site of the RdRp included Nucleoside Reverse Transcriptase Inhibitors, abacavir, emtricitabine, zidovudine, and tenofovir. Existing or new combinations of antiretroviral drugs could potentially prevent or ameliorate the course of COVID-19 if shown to inhibit SARS-CoV-2 *in vitro* and in clinical trials. Further studies are needed to establish the activity of ARVs for treatment or prevention of SARS-CoV-2 infection.

Keywords

SARS-CoV-2; COVID-19; HIV; docking; antiretrovirals; PrEP

[*]Correspondence: Dr. Douglas F. Nixon, Division of Infectious Diseases, Weill Cornell Medicine, Cornell University, Belfer Research Building, Room 530, 413 E. 69th St., New York, NY, 10021, USA. dnixon@med.cornell.edu.

[#]Equal contributors

Declarations:

Dr. Wilkin has received research funds (paid to Weill Cornell) and served as an ad hoc consultant for GlaxoSmithKline/ViiV Healthcare.

All other authors declare no conflict of interest

1.0. Introduction

The novel coronavirus, SARS-CoV-2, was first reported as a new viral infection in humans in late 2019, and over the course of 2020 the viral infection has become a pandemic. Coronavirus disease, COVID-19, has in turn taken the lives of more than 2,477,000 people by February 2021, with hundreds of thousands of more deaths expected in the absence of effective treatments or additional control measures. COVID-19 presents a major worldwide public health emergency. Only three drugs have been given emergency use authorization for use against COVID-19 in the USA, and intense research efforts are underway to find effective antiviral treatments via novel drug design or drug repurposing (Duarte et al., 2020; Elmezayen, Al-Obaidi, Sahin, & Yelekci, 2020; Sanders, Monogue, Jodlowski, & Cutrell, 2020). Many *in silico* methods have already been employed for their potential to discover repurposed drugs with activity towards SARS-CoV-2 (Aanouz et al., 2020; Boopathi, Poma, & Kolandaivel, 2020; Elmezayen et al., 2020; Enayatkhani et al., 2020; Enmozhi, Raja, Sebastine, & Joseph, 2020; Gupta et al., 2020; Hasan et al., 2020; Joshi et al., 2020; Sarma et al., 2020), including ARVs used in HIV infection, with variable results (Muralidharan, Sakthivel, Velmurugan, & Gromiha, 2020; Pant, Singh, Ravichandiran, Murty, & Srivastava, 2020) (Khan, Zia, Ashraf, Uddin, & Ul-Haq, 2020). Some studies found no change in morbidity or mortality (Byrd et al., 2020; Harter et al., 2020; Karmen-Tuohy et al., 2020), but others have observed lower SARS-CoV-2 infection rates, or lower hospitalizations in PLWH who take certain Antiretroviral drugs (ARV) regimens, like tenofovir/emtricitabine, (TDF/FTC) or Truvada (Del Amo et al., 2020). In addition, a South African study also observed a lower mortality rate for those taking tenofovir/emtricitabine although potential confounders such as healthier people taking tenofovir/emtricitabine create a channeling bias which needs to be further investigated (Boulle et al., 2020).

Antiretroviral drugs (ARVs), normally used to treat HIV infection, have also been tested in Hepatitis B Virus (HBV) infection (Boettiger et al., 2016), and in Amyotrophic Lateral Sclerosis (ALS) [NCT02437110]. ARVs have been studied *in silico*, *in vitro* and *in vivo* for their activity against Severe Acute Respiratory Syndrome (SARS) (Chu et al., 2004; Elfiky & Azzam, 2020; Yamamoto et al., 2004), and Middle East Respiratory Syndrome (MERS) (de Wilde et al., 2014), which led to adoption of two ARVs, lopinavir and ritonavir, as putative antiviral drugs against SARS-CoV-2. However, a small randomized controlled clinical trial of lopinavir and ritonavir co-administered to hospitalized adults with severe COVID-19 showed no clinical benefit over the standard of care (Cao et al., 2020), and a large randomized, controlled, open-label trial (RECOVERY), showed no clinical benefit for COVID-19 (Recovery-Collaborative-Group, 2020). For other ARVs, a preprint reported that tenofovir and emtricitabine acted as chain terminators in the replication of viral RNA by the SARS-CoV-2 RdRp (Jockusch et al., 2020). Other *in vitro* studies have also shown that ARVs such as tenofovir and abacavir are capable of terminating RNA synthesis catalyzed by the RdRp of SARS-Cov-2 as well, whereas lamivudine and emtricitabine were poor substrates for the RdRp (Chien et al., 2020). Remdesivir is approved for use by the FDA for its ability to act as a chain terminator of the growing RNA strands catalyzed by the SARS-CoV-2 RdRp. In this context, *in silico* studies can help to gauge projected mechanisms and likely molecules which bind to key viral targets, in a cost effective, high throughput manner,

whereas *in vitro* studies provide necessary details for effective inhibitory concentrations of compounds tested, and clinical studies would provide evidence for effectiveness in people.

Here, we describe a comprehensive in silico analysis of the binding of known ARVs to the catalytically active sites of the Main protease (Mpro) (PDB ID: 6Y2E) (Zhang et al., 2020) and RNA dependent RNA polymerase (RdRp) (PDB ID: 6M71) (Gao et al., 2020) of SARS-CoV-2 at atomic resolution. We used the Schrodinger's induced fit docking algorithm and molecular dynamics (MD) to identify specific HIV ARVs that could inhibit the viral replication cycle of SARS-CoV-2 by binding to these essential proteins. Results from these analyses suggest the SARS-CoV-2 Mpro is stably bound by both protease inhibitors (PI) atazanavir and indinavir. The ARVs predicted from the same protocol to bind the catalytic site of the RdRp include NRTIs, abacavir, emtricitabine, tenofovir and zidovudine.

Our results suggest that some commonly used ARVs have binding potential in silico to SARS-CoV-2 including ARVs commonly given to people without HIV as PrEP, or also used in the treatment of chronic HBV infection. Further studies should explore the activity of ARVs in vitro, in animal models, and in clinical trials, to assess whether the ARVs we identified could be used either in COVID-19 treatment regimens or as pre-exposure prophylaxis for SARS-CoV-2 infection.

2. 0. Materials and Methods

2.1 Methods overview

Maestro (v12.2.012, release 2019–4, Schrödinger) software was used to facilitate small molecule docking calculations involving high throughput virtual screening (HTVS), including flexible Induced Fit Docking (IFD), and scoring with the Glide XP (extra precision) (Friesner et al., 2006) docking score (Schrödinger, 2020, USA). Select HIV ARVs were downloaded in their active forms from the ZINC database, and PubChem when not available via ZINC. These structures were then processed using LigPrep. All defaults parameters were used, including retaining specified chiralities while varying other chiral centers.

2.2 Protein Preparation and Ligand Preparation

The main protease (Mpro) (Protein Data Bank [PDB] ID: 6Y2E) Cryo-EM structure, and the RNA-dependent RNA polymerase (RdRp) (PDB ID: 6M71) crystal structure, of SARS-Cov-2 were used for the entirety of this work. The ligand docking sites were specified as the catalytically active sites by Zhang et al. (Zhang et al., 2020) and Gao et al. (Gao et al., 2020), using an inner box distance of 10Å around the catalytically active sites, and outer box was set to automatic determination. 6Y2E's waters were separated and were not included in further analysis. The protein preparation wizard (Schrödinger) was used on its default settings to prepare both proteins. Hydrogen bonds were assigned and optimized, and a restrained minimization was carried out, using the OPLS3e forcefield (Roos et al., 2019).

Ligand Preparation was carried out using LigPrep in Maestro interface. As stated above, all HIV ARVs were downloaded as SDF files in their active forms from the ZINC database (Irwin & Shoichet, 2005), and PubChem (Kim et al., 2021) when not available via ZINC.

The OPLS3e force field was applied. Ionization was carried out using Epik (Shelley et al., 2007), at a target of pH 7.0 +/− 2.0. Desalting was allowed, and tautomers were generated. The stereoisomers were set to retain specified chiralities while varying unspecified chiral centers.

2.3 Protein-Ligand Small Molecule Docking using Schrodinger's Maestro interface

In order to identify potential binders of HIV ARVs to the catalytic sites of the SARS-COV-2 Mpro and RdRp enzymes, we performed in silico molecular docking analyses using Schrodinger's induced fit docking (IFD) followed by Glide XP docking. In the molecular structure of the Mpro (PDB ID: 6Y2E) the catalytic site is marked by residues Gln189, His41 and Cys145 (Zhang et al., 2020). For the RdRp structure (PDB ID: 6M71) the substrate binding site is marked by residues 753-FSMMILSDDAVVCFN-767 that includes the motif 759-SDD-761, which is conserved amongst polymerases (Gao et al., 2020).

2.4 Induced Fit Docking

The enzymes' catalytic sites were selected based on the residues cited above and ligands were allowed to dock within 20 Å of these sites. The side chains were refined and then optimized if docked within 5 Å of the ligands pose. Redocking was done for structures within 30kcal/mol of the best structure and within the top 20 structures overall with extra precision. Ligands were docked flexibly. The top 20 poses for each ligand were allowed, but only the top 5 poses for each were used for ranking according to their emodel score. The Glide XP docking score was then used to rank the top 5 dock for each ligand. Following selection of the molecule with the most negative emodel score, ligands were ranked according to their Glide XP scores. There was an exception to this ranking system. Indinavir had an emodel score difference of 0.8, but a docking score 2 points more negative for the pose with the slightly more positive emodel score. No other ligands fit this scoring discrepancy. Because of this, and because it was the highest scoring ligand both poses were used for MD analysis, and the one with the superior docking score was far more stable over time in the binding pocket, and is the dock pose we discuss further in the paper.

2.5 Molecular Dynamics

The unliganded Mpro and RdRp were used as references for MD analysis. In addition, the top 3 scoring ligands for the Mpro, and the top 3 ligands for the RdRp were chosen based on their IFD docking scores, and by their known mechanism of action in HIV. We also added tenofovir to this analysis, despite being the 5th ranked according to docking score, due to its reported *in vitro* activity in this paper, and proposed potential in several clinical trials (Ayerdi et al., 2020; Chien et al., 2020; Del Amo et al., 2020). These 7 top docked structures were used for further analyses due to these known properties and their simulated docking scores. This includes the RdRp docked to abacavir, emtricitabine and zidovudine and the Mpro docked to indinavir, amprenavir, and atazanavir. A 250 ns MD simulation was performed with each docked structure with Desmond (D. E. Shaw Research, New York) to assess the stability of bound structures to their target enzymes. The system was solved in a TIP3P water model and 0.15 M NaCl. Neutralization of the protein-ligand complex system was achieved by adding Na+ or Cl− counterions that balanced the net charge of the system. The full system energy minimization step was completed. The MD simulation was run for

250 ns at 300 K temperature and standard pressure (1.01325), within an orthorhombic box with buffer dimensions of 10 Å × 10 Å × 10 Å and the NPT ensemble class. The energy of 1.2 (kcal/mol) was recorded at intervals of every 100 ps resulting in 2,501 frames for each simulation. The simulations were then loaded into Maestro, for visualization of the protein ligands structures over time. The Nose-Hoover chain was used to sustain temperature at 300K. The Martyna-Tobias-Klein dynamic algorithm was used to sustain the pressure at 1.01325 bar. The simulation interaction diagram in Maestro was utilized to depict results captured in MD simulations. The final docked structures were always the reference frame used across all MD simulations and are the structures represented at time 0.

2.6 Prime MM-GBSA free energy calculations

Schrodinger's Prime MM-GBSA version 3 (Shivakumar et al., 2010) was used to calculate the free energy of binding for the 7 protein-ligand models. Specifically, the free energy of binding was calculated at 1-ns resolution, for each of the 250 ns simulations. The average free energy of binding and related standard deviations are reported in Table 3 and Table 4.

2.7 Data controls and interpretation

Because remdesivir is approved for COVID-19 treatment and has been shown in *in vitro* and *in vivo* to inhibit the SARS-CoV-2 RdRp, we used its docking score as the positive control for reporting our results (Beigel et al., 2020; Gordon et al., 2020). Remdesivir has an EC_{50} of 0.77 μM against SARS-CoV-2 viral replication in vitro (M. Wang et al., 2020). We also used boceprevir as a positive control, as it has been shown to have *in vitro* activity against the Mpro. Boceprevir has an IC_{50} of 4.13 μM, and an EC_{50} of 1.90 μM against the SARS-CoV-2 virus (Ma et al., 2020). The image portrayed in Figure 1 was created using BioRender.

3.0. Results

3.1. Estimates of COVID-19 and HIV infection

There are several important issues that complicate the issue of COVID-19 and HIV co-infection, and in the USA, PLWH of color are disproportionally impacted by COVID-19. In addition, half of PLWH in the USA are over 50 years of age, and co-morbidities are more common in this group. We estimated the number of PLWH at risk for death from COVID-19 in the USA by August 4th 2020, based upon projected estimates (Supplemental Table 1). These estimates are confounded by many variables, and since the mortality rates are fluctuating with changing testing algorithms, and data availability, they are limited in utility, yet in order to make sense of data in any observational study, such numbers need to be estimated. An observational study to determine the incidence or disease course from SARS-CoV-2 infection in PLWH who take ARV therapy, compared to those that do not is technically challenging, and problematic because ARV therapy is the standard of care for HIV worldwide. A prospective, randomized study of anti-HIV PrEP medications to prevent COVID-19, would be more appropriate. In addition, linking COVID-19-related deaths to HIV registries could provide some of these insights as well.

3.2. Induced Fit Docking

The protocol described in Figure 1 was used to analyze the ability of HIV ARV drugs to bind to the catalytic sites of the SARS-CoV-2 main protease (Mpro) (Zhang et al., 2020) and RNA-dependent RNA polymerase (RdRp) enzyme (Gao et al., 2020). The standard deviation of results presented in Tables 1 and 2, is 1.867 for the Mpro, and 2.32 for the RdRp. See the ligand interaction diagrams in Figure 2a atazanavir and 2b indinavir, each docked to the Mpro. See also ligand interaction diagrams for abacavir, emtricitabine, tenofovir and zidovudine in Figure 3. We chose the top scoring docked ligands; in addition, we considered their known mechanism in HIV. Further, we included tenofovir in the MD analysis, due to its effect in vitro and in vivo against SARS-CoV-2 (Ayerdi et al., 2020; Chien et al., 2020; Del Amo et al., 2020). Tables 1 and 2 show the top scored ligands and their Glide XP docking scores when docked to the Mpro and RdRp respectively. The mechanism of each inhibitor against HIV is listed. Controls and other antivirals are included for comparison.

3.3 Molecular Dynamics

The unliganded Mpro was stable over time only fluctuating between an RMSD of 1.2 Å and 2.4 Å. The RMSF of all residues was between 0.4 Å and 3.2 Å. However only 3 residues have an RMSF greater than 2 Å. The unliganded RdRp has an RMSD between 1.6 Å and 3.2 Å for the entire simulation. The RMSF of the unliganded RdRp is between 0.6 Å and 5 Å. The high number in some residues, stems from the multiple subunits of the RdRp which are not connected by a single amino acid chain. The binding site residues of the RdRp, at residues near 100, and 1,000, and between 210 and 800, are stable with an RMSF ranging from 0.6 Å to 2.4 Å. See supplemental material for unliganded material. The Mpro docked with either, amprenavir, atazanavir, or indinavir, were the systems used for further MD analysis. Atazanavir was the most stable protein ligand structure over time. The Cα RMSD is very stable over time for all tested structures in Figures 4a and 4c. The ligand RMSD for the Mpro-atazanavir structure is relatively stable over the entire simulation fluctuating primarily between 1.2 Å and 3.6 Å. Atazanavir is stable inside the binding pocket throughout the entire simulation. Both the Mpro-amprenavir and Mpro-indinavir models exhibit stable Cα RMSD over time as well. But upon review of the ligand RMSD for amprenavir leads to a sharp rise in RMSD which appears to be in conjunction amprenavir's instability in the binding pocket and subsequent conformational changes which leave amprenavir outside of the catalytic site (see supplemental material). The indinavir ligand RMSD is quite variable until about 120 ns when a stable conformation is achieved. Figure 4a and 4d for atazanavir and indinavir respectively, shows that the ligands are bound to residues with RMSFs mainly around 1 Å to 2 Å. The protein-ligand interactions are seen in Figure 5a and 5b, for atazanavir and indinavir respectively. Atazanavir has a majority of its interactions with Glu 166, which has been shown to be a key residue in the proper function of the Mpro in site directed mutagenesis experiments (Cheng, Chang, & Chou, 2010). Atazanavir also interacts with His 41, Asn 142 in addition to others seen in Figure 5a. Atazanavir forms interactions for more than 30% of the simulation with sidechains and waters seen in Figure 6a. Indinavir forms less interactions than atazanavir and the interaction fraction scale is smaller for that reason in Figure 5b. Indinavir has a majority of its interactions with the key residue His 41, in addition to Thr 26, Gln 189, Asn 142, Gly

143, Met 49, and others. Indinavir forms interactions for more than 30% of the simulation with sidechains and waters seen in Figure 6b. All MD results not presented here are found in the supplemental material, including the ligand RMSF, radius of gyration, intramolecular hydrogen bonding, and SASA, MolSA and PSA.

The RdRp docked with either abacavir, emtricitabine, tenofovir, or zidovudine were the selected structures used in further MD analyses based on their docking scores and reported *in vitro*, and *in vivo* (Ayerdi et al., 2020; Chien et al., 2020; Del Amo et al., 2020). The protein RMSD of all four were completely stable over the 250 ns simulation as determined by the Cα represented blue lines in Figures 7a, 7b, 7c and 7d. Looking at each MD trajectory over time makes clear that each ligand is stable within the binding pocket and does not ever leave the binding site during the 250 ns simulation. The ligand RMSD of each structure was variable, with tenofovir having the most stable ligand RMSD throughout the simulation shown in Figure 7c. Abacavir was stable until 100ns, when a sharp conformational change occurs, and a stable conformer is achieved. Emtricitabine's ligand RMSD in Figure 7b increases for 25 ns, followed by an overall relatively stable conformation throughout the remainder of the time. The zidovudine ligand RMSD has a slow increase until about 75 ns when a stable conformation is achieved, and which remains for the remainder of the 250 ns. The RMSF of each protein-ligand structure is shown in Figures 7e, 7f, 7g and 7h. Interacting residues form interactions with residues which consistently have lower RMSFs; interacting residues can be seen in detail in Figures 8 and 9. Interactions which occur for more than 30% of the simulation are seen in Figure 9. All MD results are found in the supplemental material, and include the ligand RMSF, radius of gyration, intramolecular hydrogen bonding, and SASA, MolSA and PSA.

3.4 MM-GBSA

Molecular mechanics with generalized born surface area and solvent accessibility (MM-GBSA), was used to assess the binding affinity of each structure assessed in the MD analysis, across the 250 ns simulation. The Mpro-atazanavir structure was by far the strongest binder according to its $\Delta G_{binding}$ of −86.19 kcal/mol, followed by indinavir −51.44 kcal/mol (Table 3). The strongest binder for the RdRp was abacavir with $\Delta G_{binding}$ −105.02 kcal/mol, followed closely by emtricitabine at −102.23 kcal/mol, then tenofovir at −96.70 kcal/mol, and zidovudine −93.48 kcal/mol (Table 4).

3.5 Data Availability

Remaining structural files, of docked ligands relating to the lower Glide XP scored conformers, and their subsequent poses will be made available upon request to the authors of this paper.

4. 0. Discussion

The data presented here, along with anecdotal evidence and recent *in vitro* studies, present a case for the possible prevention and treatment of COVID-19 with repurposed HIV ARV drugs. HIV ARVs were studied in past human coronavirus infections of SARS-CoV and MERS (Ford et al., 2020), and are being used in SARS-CoV-2 clinical trials as listed

in Table 5 and Table 6. Recent publications assessing COVID-19 and HIV coinfection have suggested a decreased mortality amongst some PLWH taking certain ARVs such as TDF/FTC, while others show very little difference in PLWH with no other comorbidities (Ayerdi et al., 2020; Boulle et al., 2020; Del Amo et al., 2020). In addition, two clinical trials assessing lopinavir and ritonavir failed to show any clinical benefit in people with COVID-19 (Cao et al., 2020; Recovery-Collaborative-Group, 2020). In order to better determine potential mechanistic reasons for such associations we explored the potential binding of these HIV ARVs to the known active sites of the Mpro and RdRp of SARS-CoV-2. We used chemoinformatic analyses to predict which ARVs would bind to the SARS-CoV-2 Mpro or RdRp enzymes and identified a number of compounds with predicted binding ability. Future *in vitro* work should be guided by the in-silico data present here. While further studies are needed to establish the value of ARVs in COVID-19, existing or new combinations of ARV regimens for preventing or treating HIV infection could potentially prevent or ameliorate the course of COVID-19.

The rationale supporting our work lies in previously published work describing similarities between the RNA-dependent RNA polymerase's from previous coronaviruses, including SARS, and the HIV reverse transcriptase (RT) (Oberg, 2006). Because of that similarity, ARVs were tested in the setting of SARS infection (Chu et al., 2004). SARS-CoV and SARS-CoV-2 Mpro are 96% identical (Chen, Yiu, & Wong, 2020), and SARS-CoV and the SARS-CoV-2 RdRp 98% (Shannon et al., 2020). The similarity between the enzymes of SARS-CoV and SARS-CoV-2 is marked and provided the rationale for testing drugs which were effective *in vitro* against SARS-CoV, in the setting of SARS-CoV-2 as experimental therapies.

Both the RdRp and the Mpro were analyzed by MD in their unliganded forms. Both structures had very stable RMSDs over the 250 ns MD simulations. The RdRp has a few small chains which become detached, but the overall structure is stable with no changes in conformation observed. In our IFD study presented here, indinavir was the most efficient binder and surpassed all controls with known binding affinity by the IFD analysis. However, atazanavir was the most stable in the MD analysis over the 250 ns simulation with very little variation (Figures 2a, 3a, and 4a). Atazanavir was also the most efficient binder according to MM-GBSA, with a $\Delta G_{binding}$ of −86.19. In comparison indinavir's $\Delta G_{binding}$ is −51.44. See Table 3. We hope that our results will encourage *in vitro* studies to test if indinavir or atazanavir are active against the SARS-CoV-2 Mpro. In our study amprenavir was also predicted to be a good binder by IFD, but according to the MD analysis, was very unstable in the catalytic site of the Mpro and made few interactions which sustained the length of the MD simulation. Despite this, both drugs could still be tested further *in vitro*, although widespread use of protease inhibitors would be challenging to implement because of adverse drug-drug interactions and tolerability issues.

We used boceprevir as a positive control in the IFD analysis, due to reported *in vitro* activity against the Mpro. Boceprevir has an IC_{50} of 4.13 μM, and an EC_{50} of 1.90 μM against the SARS-CoV-2 virus (Ma et al., 2020). Remdesivir, an adenosine nucleotide analogue currently with emergency FDA-approval for COVID-19 treatment, has activity against the RdRp of SARS-CoV-2 (Gordon et al., 2020) by incorporation into the growing

RNA strand and inhibiting further viral transcription. Remdesivir was the first agent to show clinical efficacy in a randomized (Beigel et al., 2020) placebo-controlled study. However, more accessible oral drugs would help expand the antiviral drug range. Tenofovir and emtricitabine can inhibit the RdRp of SARS-CoV-2 *in vitro* (Jockusch et al., 2020), as expected from our *in silico* analyses, and another study using a different method found both tenofovir and abacavir to be better suited than lamivudine or emtricitabine against the RdRp. Interestingly nucleotide reverse transcriptase inhibitors like emtricitabine and lamivudine are –(−) nucleotides, and are the mirror image of the D-ribose nucleotides (Hung et al., 2019). They are incorporated "backwards" into growing HIV DNA primer strands in their intended HIV inhibition mechanism (Hung et al., 2019). Both nucleotide analogs and nucleoside analogs can be incorporated into growing RNA strands and thus may act as chain terminators of growing viral RNA strands under replication by the RdRp, likely due to the low fidelity of the RdRp to its substrate (Jockusch et al., 2020; McKenna, Kashemirov, Peterson, & Goodman, 2010). It should be noted that according to their work, NRTIs like tenofovir and abacavir, seem superior to others like emtricitabine and lamivudine. Our work suggests that people on a regimen containing tenofovir, emtricitabine, abacavir, lamivudine, or zidovudine, could potentially be partially protected from SARS-CoV-2 infection or COVID-19, although only additional *in vitro* studies like the one mentioned above, and clinical trials can determine this concretely. Considering the data here and the data discussed next, tenofovir seems the most likely candidate for further study.

According to our MD results, tenofovir had one of the lowest docking scores amongst the NRTIs and yet was clearly more stable than the other ligands examined by MD. Zidovudine and emtricitabine were also stable over the entire MD analysis, with only small conformational changes in the ligand conformation occurring until about 50 ns, as seen by the ligand RMSD plots in Figure 7. The MM-GBSA results show all of the ligands have good, predicted binding to the nucleoside/nucleotide (NT) binding site in Table 4. Of course, using this data to determine if these nucleotides/nucleosides will be incorporated into a growing primer RNA strand is not possible with current in silico models. Interestingly only tenofovir exhibited significant binding to the residue Asp760, which is the nucleotide binding site on the RdRp as stated above. It is the most stable of the ligands tested according to ligand RMSD in Figure 7c. Considering the clinical trials, *in vitro* work, and now this work suggesting the stability of tenofovir in the NT binding site, tenofovir is an important candidate for further study against the SARS-CoV-2 RdRp.

It is not unexpected that NNRTIs as a class did not bind well to the catalytic site for the SARS-CoV-2 RdRp, which is the NT binding site, where elongation of the RNA strand occurs (Gao et al., 2020). When NRTIs are metabolized and form triphosphate structures, they are capable of being added to the growing RNA/DNA strand and chain termination will follow (Gordon et al., 2020; Jockusch et al., 2020; Y. Wang et al., 2020). However, HIV reverse transcriptase is inhibited by NNRTIs at a site different from that which the NRTIs bind. Instead, NNRTIs inhibit HIV RT in a non-competitive fashion, binding at a site distant from the polymerase active site, usually stopping key nucleic acid-protein interactions from occurring, or changing the active site structure (Sluis-Cremer & Tachedjian, 2008). Past studies have found no potential homologous hydrophobic NNRTI binding site on the previous SARS-CoV RdRp structure (Xu et al., 2003), although we identified potential

hydrophobic pockets on the surface of the RdRp (data not shown). This will remain an area for further research to address, though COVID-19 research should certainly include second generation NNRTIs with more rotatable bonds and flexibility. If HIV NNRTIs are observed to offer potential protection it should become clear in observational or retrospective studies.

In order to better understand the impact of ARVs on SARS-CoV-2 infection or COVID-19, PLWH or people at risk of HIV infection on pre-exposure prophylaxis (PrEP) could provide critical insights into the course of COVID-19. An early report first showed that PLWH on ARVs can be infected by SARS-CoV-2 (Blanco et al., 2020), but of the first 543 people admitted to a hospital in Barcelona with COVID-19, only five were PLWH. New data has also been presented which compared over 30,000 PLWH and 76,000 matched controls and described 189 PLWH and their COVID-19 outcomes (Park LS, 2020). Additionally, registries (Dandachi et al., 2020) can also provide greater insight into the difference or lack of difference in COVID-19 outcomes amongst PLWH.

Our data suggests that select ARVs could also be tested as pre-exposure prophylaxis (PrEP) for COVID-19, if *in vitro* efficacy was shown. Drugs used for HIV PrEP (tenofovir/emtricitabine) are well tolerated (Mayer et al., 2020), and, if effective against SARS-CoV-2 *in vitro*, trials would be more easily justified given the excellent tolerability, lack of drug-drug interactions, and well characterized safety profile, when compared to PIs. We also look forward to results from planned research such as the placebo-controlled study of SARS-CoV-2 prophylaxis with tenofovir disoproxil fumarate/emtricitabine vs. hydroxychloroquine vs. both (vs placebo) in health care workers in Spain (N=4000) NCT04334928.

5. 0. Conclusions

At this time the authors of this study would like to caution that this report has not made any conclusion or recommendation to change any treatment or prevention regimen. However, our studies suggest that further investigations of the role of ARVs in SARS-CoV-2 prevention or amelioration of COVID-19 are warranted.

Supplementary Material

Refer to Web version on PubMed Central for supplementary material.

Acknowledgments

6. 0. Funding

This study was supported, in part by an NIH grant, BELIEVE (NIH grant 1UM1AI126617) for M.d.M.R. and D.F.N.; M.d.M.R. is supported by the Fund for the Future Award (Weill Cornell Medicine) granted by the Kellen Foundation.

Abbreviations:

AI	Attachment Inhibito
ALS	Amyotrophic Lateral Sclerosis

ARVs	Antiretrovirals
COVID-19	Coronavirus disease
CYP3A	Cytochrome P450, family 3, subfamily A
Glide XP	extra precision
EI	Entry Inhibitor
HBV	Hepatitis B virus
HTVS	High Throughput Virtual Screening
INSTI	Integrase Strand Transfer Inhibitor
MERS	Middle East Respiratory Syndrome
MM-GBSA	Molecular Mechanics with Generalized Born Surface Area and Solvent Accessibility
Mpro	SARS-CoV-2 Main Protease
NNRTI	Non-Nucleoside Reverse Transcriptase Inhibitor
NRTI	Nucleoside/Nucleotide Reverse Transcriptase Inhibitor
NT	Nucleoside/Nucleotide
PDB	Protein Data Bank
PI	Protease Inhibitor
PK	Pharmacokinetics
PLWH	People Living With HIV
PrEP	Pre-Exposure Prophylaxis
RdRp	SARS-CoV-2 RNA Dependent RNA Polymerase
RT	Reverse Transcriptase
SARS	Severe Acute Respiratory Syndrome
SARS-CoV-2	Severe Acute Respiratory Syndrome Coronavirus type 2

References

Aanouz I, Belhassan A, El-Khatabi K, Lakhlifi T, El-Ldrissi M, & Bouachrine M (2020). Moroccan Medicinal plants as inhibitors against SARS-CoV-2 main protease: Computational investigations. J Biomol Struct Dyn, 1–9. doi:10.1080/07391102.2020.1758790

Ayerdi O, Puerta T, Clavo P, Vera M, Ballesteros J, Fuentes ME, . . . Sandoval Study G (2020). Preventive Efficacy of Tenofovir/Emtricitabine Against Severe Acute Respiratory Syndrome Coronavirus 2 Among Pre-Exposure Prophylaxis Users. Open Forum Infect Dis, 7(11), ofaa455. doi:10.1093/ofid/ofaa455 [PubMed: 33200081]

Beigel JH, Tomashek KM, Dodd LE, Mehta AK, Zingman BS, Kalil AC, . . . Members, A.-S. G. (2020). Remdesivir for the Treatment of Covid-19 - Final Report. N Engl J Med doi:10.1056/NEJMoa2007764

Blanco JL, Ambrosioni J, Garcia F, Martinez E, Soriano A, Mallolas J, . . . Investigators, C.-i. H. (2020). COVID-19 in patients with HIV: clinical case series. Lancet HIV doi:10.1016/S2352-3018(20)30111-9

Boettiger DC, Kerr S, Ditangco R, Chaiwarith R, Li PC, Merati TP, . . . Database, T. A. H. O. (2016). Tenofovir-based antiretroviral therapy in HBV-HIV coinfection: results from the TREAT Asia HIV Observational Database. Antivir Ther, 21(1), 27–35. doi:10.3851/IMP2972 [PubMed: 26069150]

Boopathi S, Poma AB, & Kolandaivel P (2020). Novel 2019 coronavirus structure, mechanism of action, antiviral drug promises and rule out against its treatment. J Biomol Struct Dyn, 1–10. doi:10.1080/07391102.2020.1758788

Boulle A, Davies MA, Hussey H, Ismail M, Morden E, Vundle Z, . . . Tamuhla T (2020). Risk factors for COVID-19 death in a population cohort study from the Western Cape Province, South Africa. Clin Infect Dis doi:10.1093/cid/ciaa1198

Byrd KM, Beckwith CG, Garland JM, Johnson JE, Aung S, Cu-Uvin S, . . . Kantor R (2020). SARS-CoV-2 and HIV coinfection: clinical experience from Rhode Island, United States. J Int AIDS Soc, 23(7), e25573. doi:10.1002/jia2.25573 [PubMed: 32657527]

Cao B, Wang Y, Wen D, Liu W, Wang J, Fan G, . . . Wang C (2020). A Trial of Lopinavir-Ritonavir in Adults Hospitalized with Severe Covid-19. N Engl J Med doi:10.1056/NEJMoa2001282

Chen YW, Yiu CB, & Wong KY (2020). Prediction of the SARS-CoV-2 (2019-nCoV) 3C-like protease (3CL (pro)) structure: virtual screening reveals velpatasvir, ledipasvir, and other drug repurposing candidates. F1000Res, 9, 129. doi:10.12688/f1000research.22457.2 [PubMed: 32194944]

Cheng SC, Chang GG, & Chou CY (2010). Mutation of Glu-166 blocks the substrate-induced dimerization of SARS coronavirus main protease. Biophys J, 98(7), 1327–1336. doi:10.1016/j.bpj.2009.12.4272 [PubMed: 20371333]

Chien M, Anderson TK, Jockusch S, Tao C, Li X, Kumar S, . . . Ju J (2020). Nucleotide Analogues as Inhibitors of SARS-CoV-2 Polymerase, a Key Drug Target for COVID-19. J Proteome Res, 19(11), 4690–4697. doi:10.1021/acs.jproteome.0c00392 [PubMed: 32692185]

Chu CM, Cheng VC, Hung IF, Wong MM, Chan KH, Chan KS, . . . Group, H. U. S. S. (2004). Role of lopinavir/ritonavir in the treatment of SARS: initial virological and clinical findings. Thorax, 59(3), 252–256. doi:10.1136/thorax.2003.012658 [PubMed: 14985565]

Dandachi D, Geiger G, Montgomery MW, Karmen-Tuohy S, Golzy M, Antar AAR, . . . consortium, H.-C.−. (2020). Characteristics, Comorbidities, and Outcomes in a Multicenter Registry of Patients with HIV and Coronavirus Disease-19. Clin Infect Dis doi:10.1093/cid/ciaa1339

de Wilde AH, Jochmans D, Posthuma CC, Zevenhoven-Dobbe JC, van Nieuwkoop S, Bestebroer TM, . . . Snijder EJ (2014). Screening of an FDA-approved compound library identifies four small-molecule inhibitors of Middle East respiratory syndrome coronavirus replication in cell culture. Antimicrob Agents Chemother, 58(8), 4875–4884. doi:10.1128/AAC.03011-14 [PubMed: 24841269]

Del Amo J, Polo R, Moreno S, Diaz A, Martinez E, Arribas JR, . . . The Spanish, H. I. V. C.-C. (2020). Incidence and Severity of COVID-19 in HIV-Positive Persons Receiving Antiretroviral Therapy : A Cohort Study. Ann Intern Med, 173(7), 536–541. doi:10.7326/M20-3689 [PubMed: 32589451]

Duarte RRR, Copertino DC Jr, Iñiguez LP, Marston JL, Nixon DF, & Powell TR (2020). Repurposing FDA-Approved Drugs for COVID-19 Using a Data-Driven Approach. ChemRxiv doi:10.26434/chemrxiv.12148764.v1

Elfiky AA, & Azzam EB (2020). Novel guanosine derivatives against MERS CoV polymerase: An in silico perspective. J Biomol Struct Dyn, 1–9. doi:10.1080/07391102.2020.1758789

Elmezayen AD, Al-Obaidi A, Sahin AT, & Yelekci K (2020). Drug repurposing for coronavirus (COVID-19): in silico screening of known drugs against coronavirus 3CL hydrolase and protease enzymes. J Biomol Struct Dyn, 1–13. doi:10.1080/07391102.2020.1758791

Enayatkhani M, Hasaniazad M, Faezi S, Guklani H, Davoodian P, Ahmadi N, . . . Ahmadi K (2020). Reverse vaccinology approach to design a novel multi-epitope vaccine candidate against COVID-19: an in silico study. J Biomol Struct Dyn, 1–16. doi:10.1080/07391102.2020.1756411

Enmozhi SK, Raja K, Sebastine I, & Joseph J (2020). Andrographolide as a potential inhibitor of SARS-CoV-2 main protease: an in silico approach. J Biomol Struct Dyn, 1–7. doi:10.1080/07391102.2020.1760136

Ford N, Vitoria M, Rangaraj A, Norris SL, Calmy A, & Doherty M (2020). Systematic review of the efficacy and safety of antiretroviral drugs against SARS, MERS or COVID-19: initial assessment. J Int AIDS Soc, 23(4), e25489. doi:10.1002/jia2.25489 [PubMed: 32293807]

Friesner RA, Murphy RB, Repasky MP, Frye LL, Greenwood JR, Halgren TA, . . . Mainz DT (2006). Extra precision glide: docking and scoring incorporating a model of hydrophobic enclosure for protein-ligand complexes. J Med Chem, 49(21), 6177–6196. doi:10.1021/jm051256o [PubMed: 17034125]

Gao Y, Yan L, Huang Y, Liu F, Zhao Y, Cao L, . . . Rao Z (2020). Structure of the RNA-dependent RNA polymerase from COVID-19 virus. Science doi:10.1126/science.abb7498

Gordon CJ, Tchesnokov EP, Woolner E, Perry JK, Feng JY, Porter DP, & Gotte M (2020). Remdesivir is a direct-acting antiviral that inhibits RNA-dependent RNA polymerase from severe acute respiratory syndrome coronavirus 2 with high potency. J Biol Chem doi:10.1074/jbc.RA120.013679

Gupta MK, Vemula S, Donde R, Gouda G, Behera L, & Vadde R (2020). In-silico approaches to detect inhibitors of the human severe acute respiratory syndrome coronavirus envelope protein ion channel. J Biomol Struct Dyn, 1–11. doi:10.1080/07391102.2020.1751300

Harter G, Spinner CD, Roider J, Bickel M, Krznaric I, Grunwald S, . . . Hoffmann C (2020). COVID-19 in people living with human immunodeficiency virus: a case series of 33 patients. Infection, 48(5), 681–686. doi:10.1007/s15010-020-01438-z [PubMed: 32394344]

Hasan A, Paray BA, Hussain A, Qadir FA, Attar F, Aziz FM, . . . Falahati M (2020). A review on the cleavage priming of the spike protein on coronavirus by angiotensin-converting enzyme-2 and furin. J Biomol Struct Dyn, 1–9. doi:10.1080/07391102.2020.1754293

Hung M, Tokarsky EJ, Lagpacan L, Zhang L, Suo Z, & Lansdon EB (2019). Elucidating molecular interactions of L-nucleotides with HIV-1 reverse transcriptase and mechanism of M184V-caused drug resistance. Commun Biol, 2, 469. doi:10.1038/s42003-019-0706-x [PubMed: 31872074]

Irwin JJ, & Shoichet BK (2005). ZINC--a free database of commercially available compounds for virtual screening. J Chem Inf Model, 45(1), 177–182. doi:10.1021/ci049714+ [PubMed: 15667143]

Jockusch S, Tao C, Li X, Anderson TK, Chien M, Kumar S, . . . Ju J (2020). Triphosphates of the Two Components in DESCOVY and TRUVADA are Inhibitors of the SARS-CoV-2 Polymerase. BioRxiv, 2020.04.03.022939. doi:10.1101/2020.04.03.022939

Joshi RS, Jagdale SS, Bansode SB, Shankar SS, Tellis MB, Pandya VK, . . . Kulkarni MJ (2020). Discovery of potential multi-target-directed ligands by targeting host-specific SARS-CoV-2 structurally conserved main protease. J Biomol Struct Dyn, 1–16. doi:10.1080/07391102.2020.1760137

Karmen-Tuohy S, Carlucci PM, Zervou FN, Zacharioudakis IM, Rebick G, Klein E, . . . Rahimian J (2020). Outcomes Among HIV-Positive Patients Hospitalized With COVID-19. J Acquir Immune Defic Syndr, 85(1), 6–10. doi:10.1097/QAI.0000000000002423 [PubMed: 32568770]

Khan SA, Zia K, Ashraf S, Uddin R, & Ul-Haq Z (2020). Identification of chymotrypsin-like protease inhibitors of SARS-CoV-2 via integrated computational approach. J Biomol Struct Dyn, 1–10. doi:10.1080/07391102.2020.1751298

Kim S, Chen J, Cheng T, Gindulyte A, He J, He S, . . . Bolton EE (2021). PubChem in 2021: new data content and improved web interfaces. Nucleic Acids Res, 49(D1), D1388–D1395. doi:10.1093/nar/gkaa971 [PubMed: 33151290]

Ma C, Sacco MD, Hurst B, Townsend JA, Hu Y, Szeto T, . . . Wang J (2020). Boceprevir, GC-376, and calpain inhibitors II, XII inhibit SARS-CoV-2 viral replication by targeting the viral main protease. BioRxiv doi:10.1101/2020.04.20.051581

Mayer KH, Molina JM, Thompson MA, Anderson PL, Mounzer KC, De Wet JJ, . . . Hare CB (2020). Emtricitabine and tenofovir alafenamide vs emtricitabine and tenofovir disoproxil fumarate for HIV pre-exposure prophylaxis (DISCOVER): primary results from a randomised, double-

blind, multicentre, active-controlled, phase 3, non-inferiority trial. Lancet, 396(10246), 239–254. doi:10.1016/S0140-6736(20)31065-5 [PubMed: 32711800]

McKenna CE, Kashemirov BA, Peterson LW, & Goodman MF (2010). Modifications to the dNTP triphosphate moiety: from mechanistic probes for DNA polymerases to antiviral and anti-cancer drug design. Biochim Biophys Acta, 1804(5), 1223–1230. doi:10.1016/j.bbapap.2010.01.005 [PubMed: 20079885]

Muralidharan N, Sakthivel R, Velmurugan D, & Gromiha MM (2020). Computational studies of drug repurposing and synergism of lopinavir, oseltamivir and ritonavir binding with SARS-CoV-2 protease against COVID-19. J Biomol Struct Dyn, 1–6. doi:10.1080/07391102.2020.1752802

Oberg B (2006). Rational design of polymerase inhibitors as antiviral drugs. Antiviral Res, 71(2–3), 90–95. doi:10.1016/j.antiviral.2006.05.012 [PubMed: 16820225]

Pant S, Singh M, Ravichandiran V, Murty USN, & Srivastava HK (2020). Peptide-like and small-molecule inhibitors against Covid-19. J Biomol Struct Dyn, 1–10. doi:10.1080/07391102.2020.1757510

Park LS RC, Sigel K, et al. . (2020). COVID-19 in the largest US HIV cohort Paper presented at the AIDS 2020: 23rd International AIDS Conference Virtual.

Recovery-Collaborative-Group. (2020). Lopinavir-ritonavir in patients admitted to hospital with COVID-19 (RECOVERY): a randomised, controlled, open-label, platform trial. Lancet doi:10.1016/S0140-6736(20)32013-4

Roos K, Wu C, Damm W, Reboul M, Stevenson JM, Lu C, . . . Harder ED (2019). OPLS3e: Extending Force Field Coverage for Drug-Like Small Molecules. J Chem Theory Comput, 15(3), 1863–1874. doi:10.1021/acs.jctc.8b01026 [PubMed: 30768902]

Sanders JM, Monogue ML, Jodlowski TZ, & Cutrell JB (2020). Pharmacologic Treatments for Coronavirus Disease 2019 (COVID-19): A Review. JAMA doi:10.1001/jama.2020.6019

Sarma P, Shekhar N, Prajapat M, Avti P, Kaur H, Kumar S, . . . Medhi B (2020). In-silico homology assisted identification of inhibitor of RNA binding against 2019-nCoV N-protein (N terminal domain). J Biomol Struct Dyn, 1–9. doi:10.1080/07391102.2020.1753580

Shannon A, Le NT, Selisko B, Eydoux C, Alvarez K, Guillemot JC, . . . Canard B (2020). Remdesivir and SARS-CoV-2: Structural requirements at both nsp12 RdRp and nsp14 Exonuclease active-sites. Antiviral Res, 178, 104793. doi:10.1016/j.antiviral.2020.104793 [PubMed: 32283108]

Shelley JC, Cholleti A, Frye LL, Greenwood JR, Timlin MR, & Uchimaya M (2007). Epik: a software program for pK(a) prediction and protonation state generation for drug-like molecules. J Comput Aided Mol Des, 21(12), 681–691. doi:10.1007/s10822-007-9133-z [PubMed: 17899391]

Shivakumar D, Williams J, Wu Y, Damm W, Shelley J, & Sherman W (2010). Prediction of Absolute Solvation Free Energies using Molecular Dynamics Free Energy Perturbation and the OPLS Force Field. J Chem Theory Comput, 6(5), 1509–1519. doi:10.1021/ct900587b [PubMed: 26615687]

Sluis-Cremer N, & Tachedjian G (2008). Mechanisms of inhibition of HIV replication by non-nucleoside reverse transcriptase inhibitors. Virus Res, 134(1–2), 147–156. doi:10.1016/j.virusres.2008.01.002 [PubMed: 18372072]

Wang M, Cao R, Zhang L, Yang X, Liu J, Xu M, . . . Xiao G (2020). Remdesivir and chloroquine effectively inhibit the recently emerged novel coronavirus (2019-nCoV) in vitro. Cell Res, 30(3), 269–271. doi:10.1038/s41422-020-0282-0 [PubMed: 32020029]

Wang Y, Zhang D, Du G, Du R, Zhao J, Jin Y, . . . Wang C (2020). Remdesivir in adults with severe COVID-19: a randomised, double-blind, placebo-controlled, multicentre trial. The Lancet, 0(0). doi:10.1016/s0140-6736(20)31022-9

Xu X, Liu Y, Weiss S, Arnold E, Sarafianos SG, & Ding J (2003). Molecular model of SARS coronavirus polymerase: implications for biochemical functions and drug design. Nucleic Acids Res, 31(24), 7117–7130. doi:10.1093/nar/gkg916 [PubMed: 14654687]

Yamamoto N, Yang R, Yoshinaka Y, Amari S, Nakano T, Cinatl J, . . . Yamamoto N (2004). HIV protease inhibitor nelfinavir inhibits replication of SARS-associated coronavirus. Biochem Biophys Res Commun, 318(3), 719–725. doi:10.1016/j.bbrc.2004.04.083 [PubMed: 15144898]

Zhang L, Lin D, Sun X, Curth U, Drosten C, Sauerhering L, . . . Hilgenfeld R (2020). Crystal structure of SARS-CoV-2 main protease provides a basis for design of improved alpha-ketoamide inhibitors. Science doi:10.1126/science.abb3405

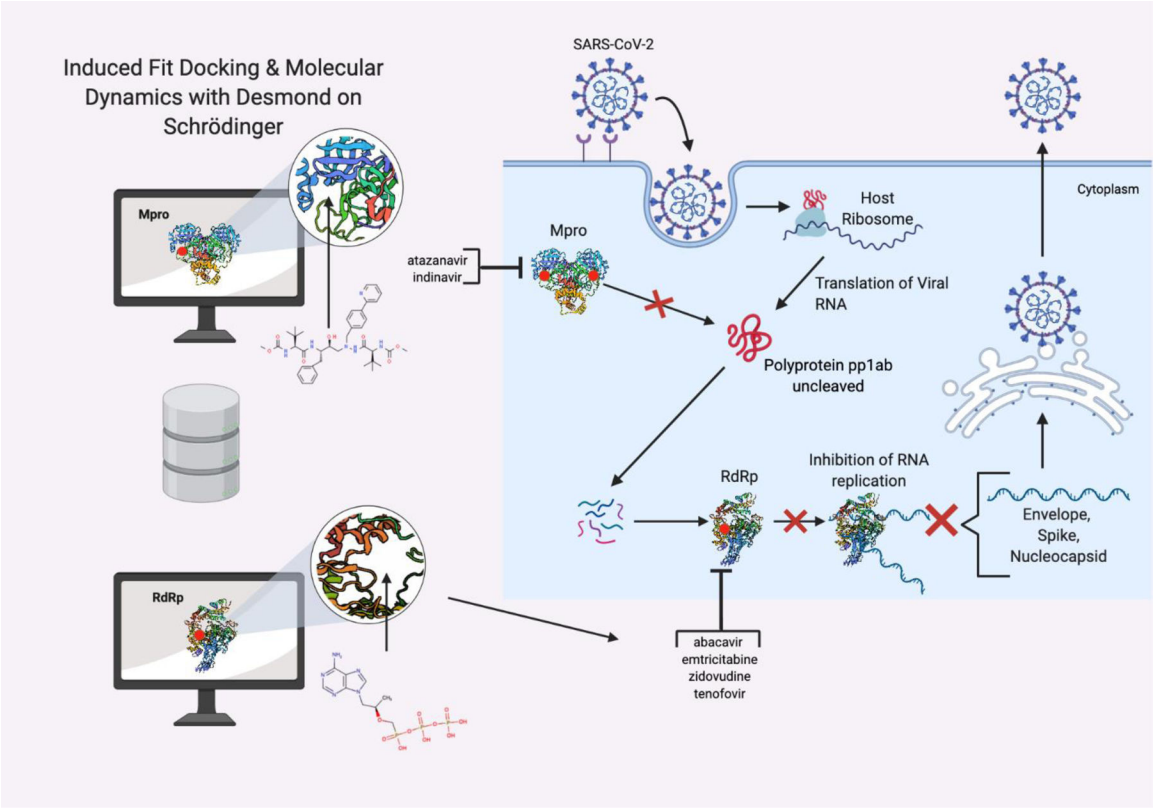

Figure 1.

Overall schematic for the methods used in this paper and our significant results. Molecules are docked to key residues of the viral enzymes. The HIV ARVs that are predicted to bind to designated catalytic sites of the viral enzymes are those listed next to either bracket. The red dots indicate the designated catalytic sites for the purpose of this study. The binding and potential inhibition of these enzymes would disrupt the replication machinery of this virus, as shown by the replication schematic.

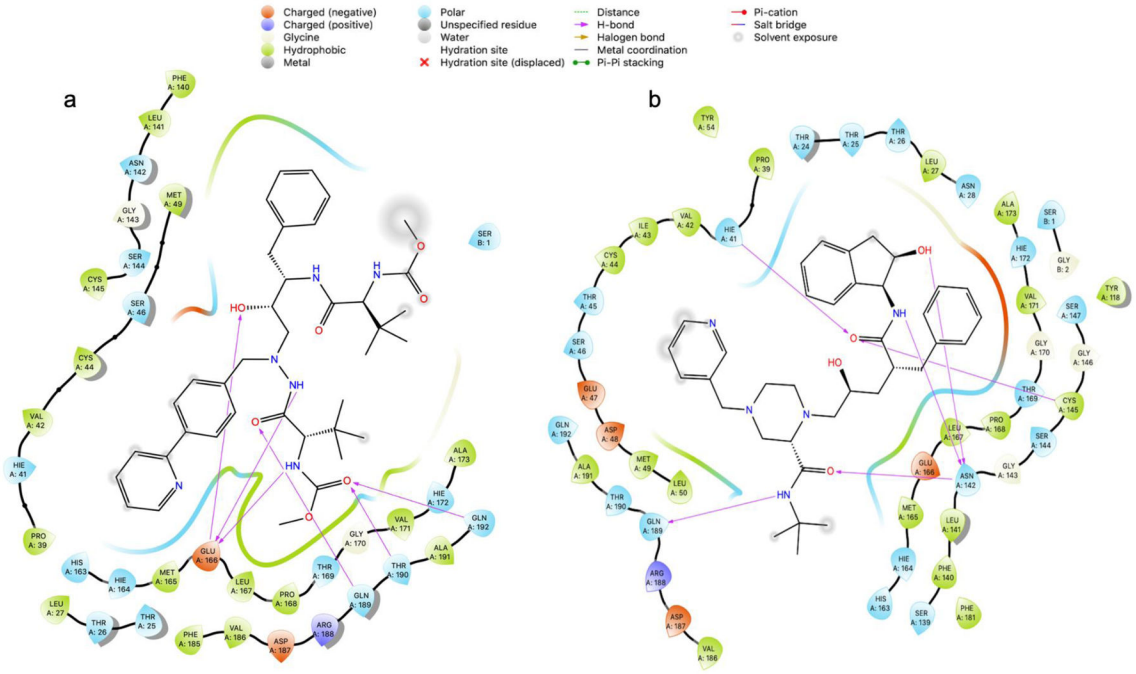

Figure 2.

Ligand interaction diagrams in 2D from induced fit docking of (a) atazanavir, and (b) indinavir to the Mpro.

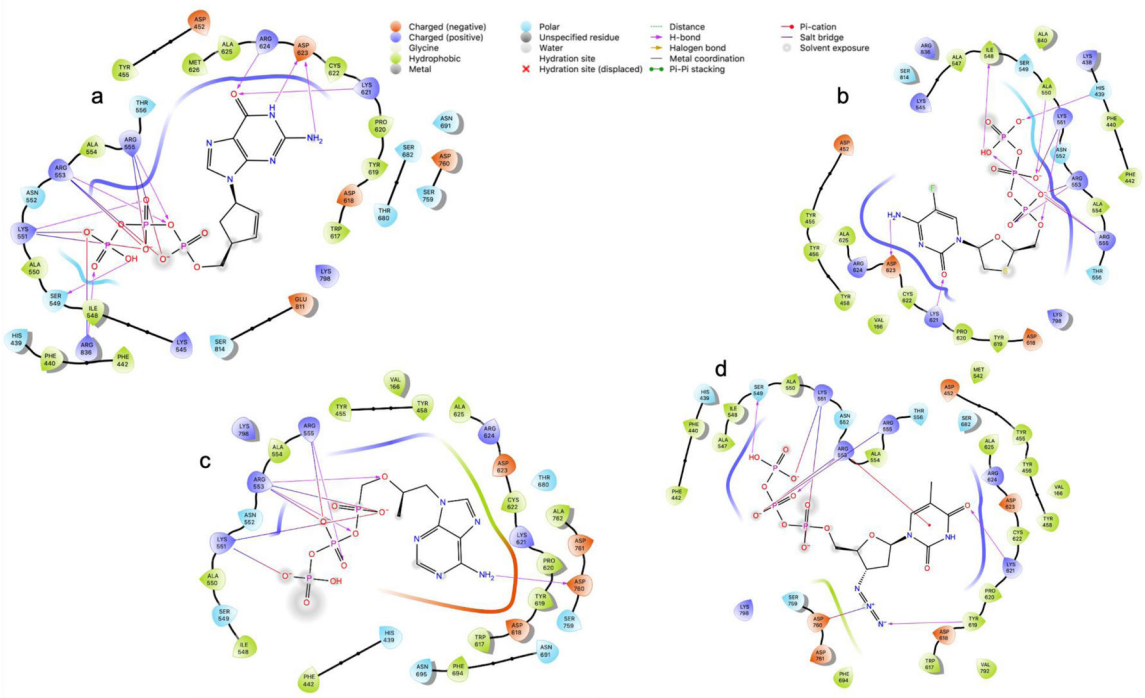

Figure 3.

Ligand interaction diagrams in 2D from induced fit docking of (a) abacavir, (b) emtricitabine, (c) tenofovir, and (d) zidovudine.

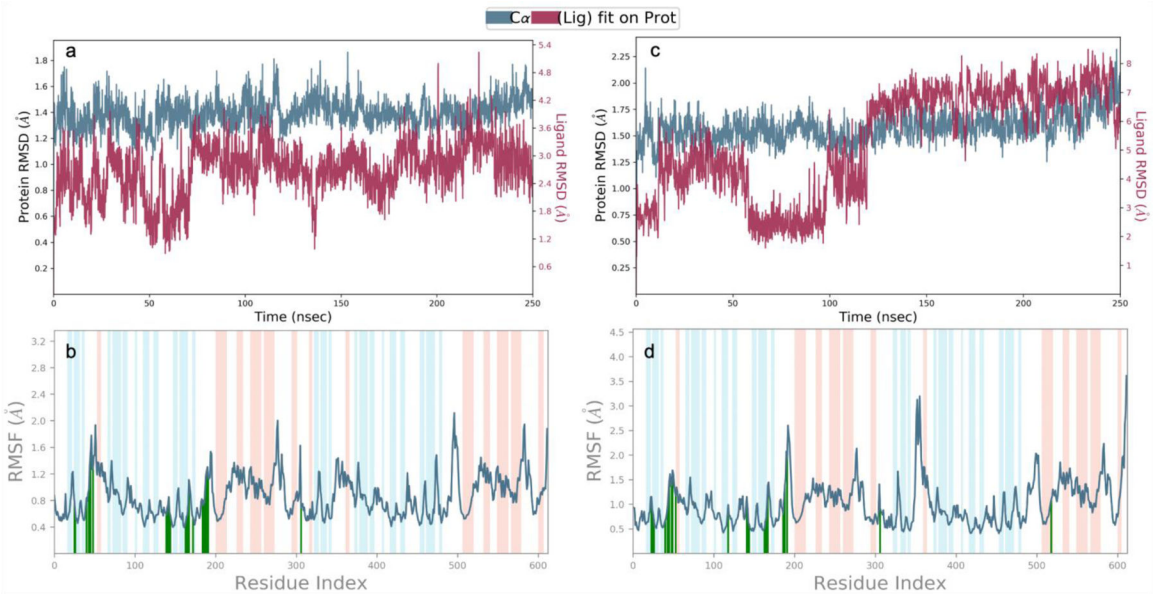

Figure 4.

Protein-ligand RMSD plots for the Mpro, (a) atazanavir, and (c) indinavir complexes. For Cα atoms of the Mpro the RMSD is represented by the blue line (scale on left). The RMSD of the ligands are represented by the red line with the scale to the right of the figures in the top row. Please note that all graphs have various scales. The x-axis scale is in nanoseconds, the y-axis is in Angstroms. Protein RMSF plots in bottom row, of (b) atazanavir, and (d) indinavir complexed with Mpro. Secondary structural elements of alpha helices and beta strands are represented by highlighted red and blue backgrounds respectively. Protein ligand contacts are marked with green vertical bars. Please note the varying scales used in each graph.

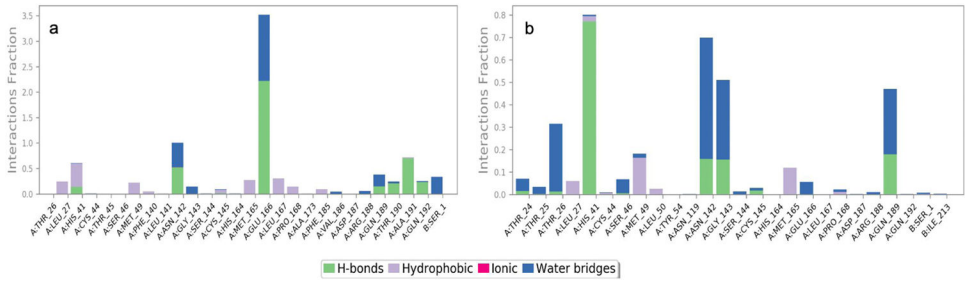

Figure 5.

Protein ligand contacts of the Mpro with the (a) atazanavir, and (b) indinavir ligands respectively. Hydrogen bonds represented in green, purple representing hydrophobic interactions, pink for ionic, and blue for water bridges.

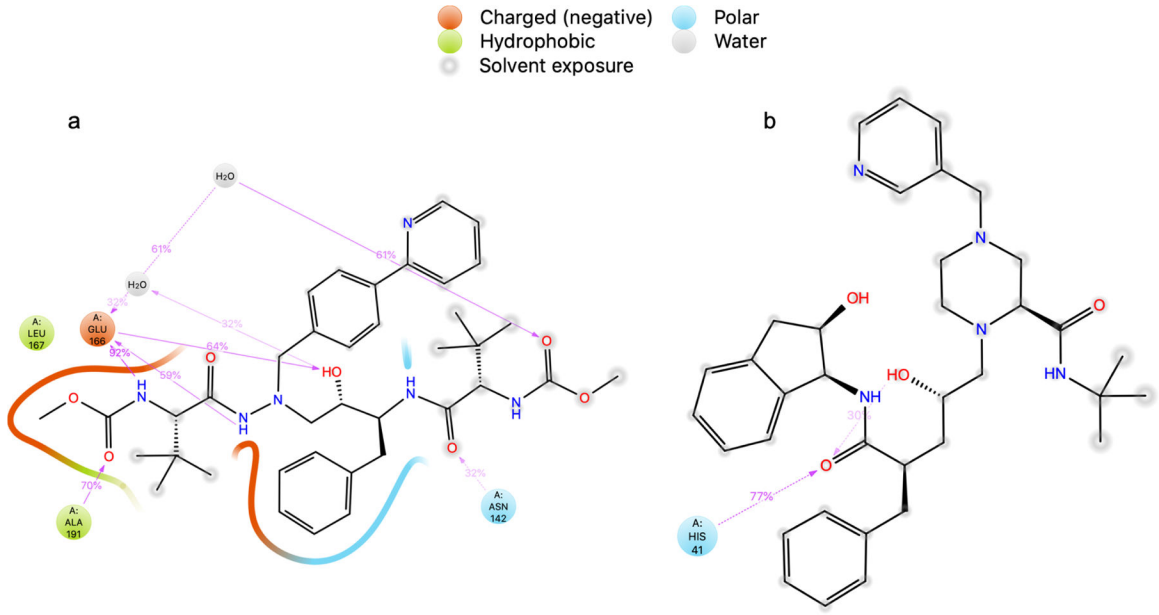

Figure 6.

Detailed protein ligand interactions which occur over time in the MD simulation are shown for (a) atazanavir, and (b) indinavir. Only interactions which occur for more than 30% of the simulation are shown in each.

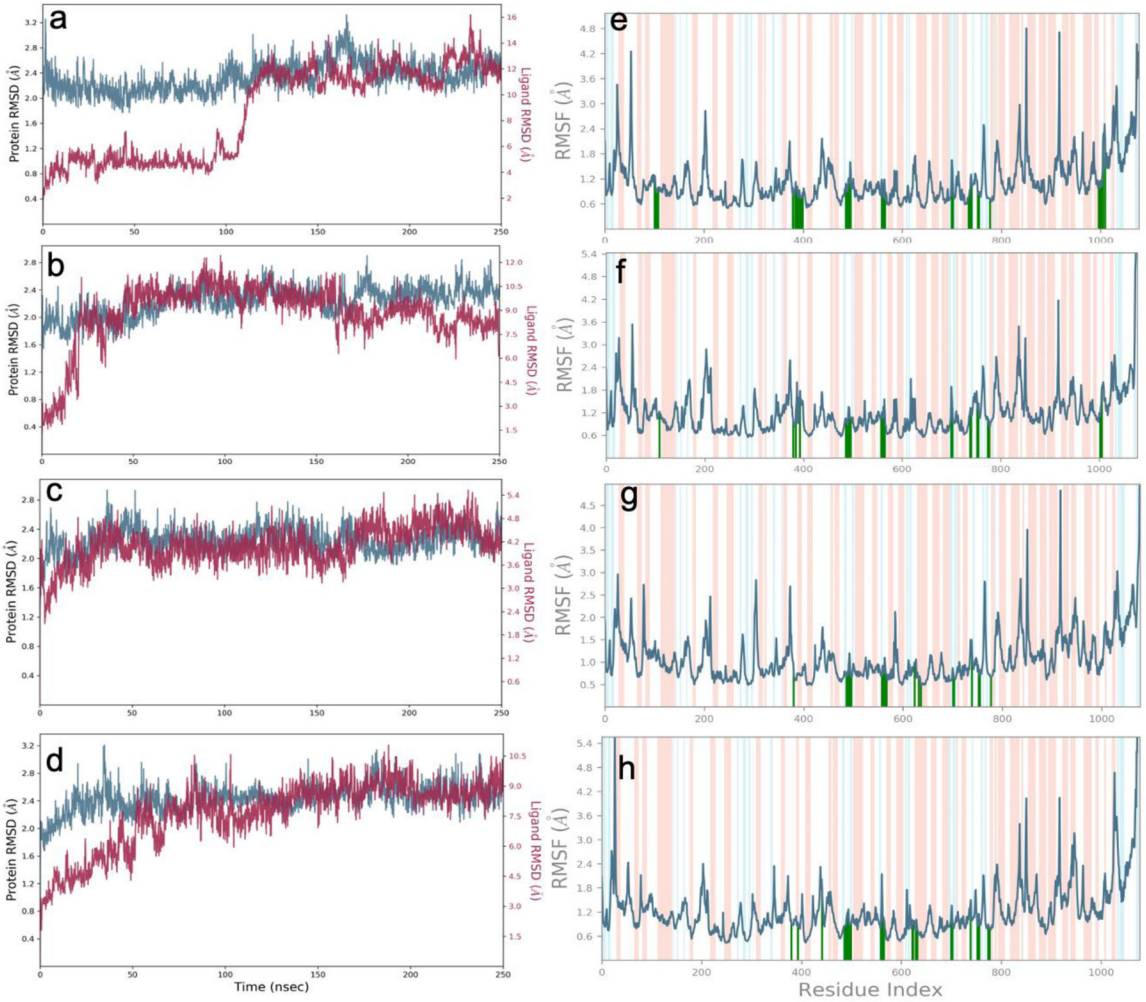

Figure 7.

RMSD plots in left column, for the Cα (blue, scale left) from MD analysis of RdRp (a) abacavir, (b) emtricitabine, (c) tenofovir, and (d) zidovudine complexes. The ligand RMSD plot (magenta, scale right). Protein RMSF plots in right column, of (e) abacavir, (f) emtricitabine, (g) tenofovir, and (h) zidovudine complexed with RdRp. Secondary structural elements of alpha helices and beta strands are represented by highlighted red and blue backgrounds respectively. Protein ligand contacts are marked with green vertical bars. Please note the varying scales in each graph.

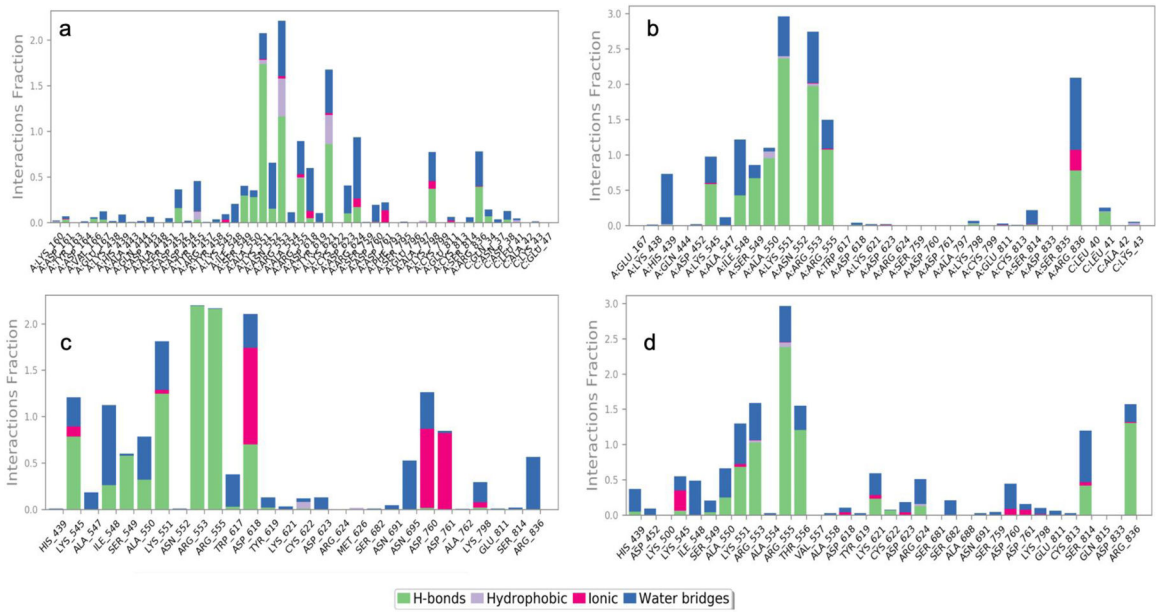

Figure 8.

Protein ligand contacts of the RdRp with the (a) abacavir, (b) emtricitabine, (c) tenofovir, and (d) zidovudine ligands respectively. Hydrogen bonds represented in green, purple representing hydrophobic interactions, pink for ionic, and blue for water bridges.

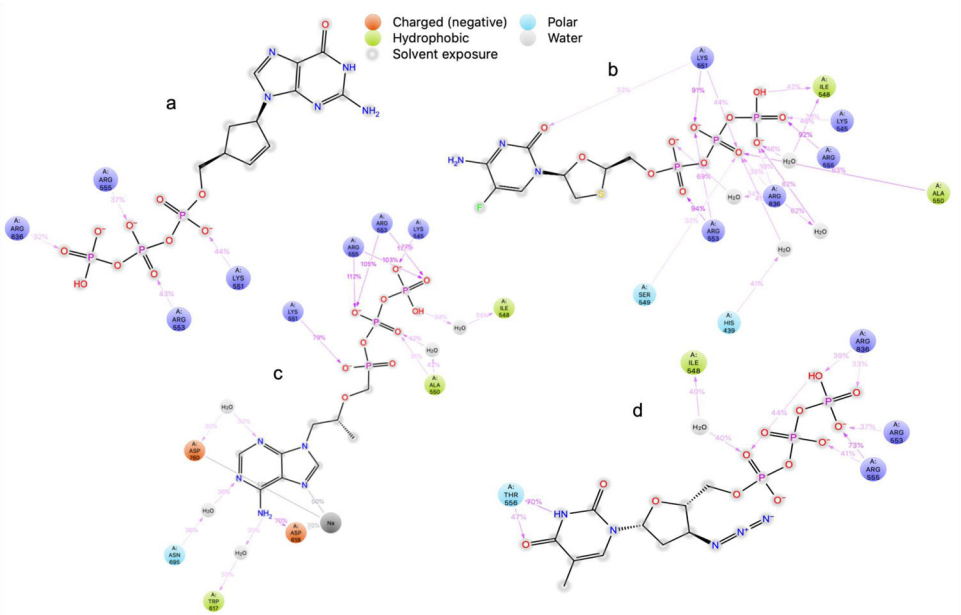

Figure 9.

Detailed protein ligand interactions which occur over time in the MD simulation are shown for the RdRp- (a) abacavir, (b) emtricitabine, (c) tenofovir, and (d) zidovudine complexes. Only interactions which occur for at least 30% of the simulation are shown in each. For more detailed interactions across each please see the supplemental material.

The Glide XP docking scores utilize an empirical scoring function which approximates the ligand binding free energy, when the ligands bind to the designated catalytic sites of either the Mpro or RdRp. More negative numbers suggest more free energy associated with the predicted binding event (Table 1, Table 2).

Table 1.

Docking scores for HIV drugs tested against SARS-CoV-2 Mpro. The HIV ARV inhibitor class is also referenced (below).

Drug Name	Glide XP Score	Drug Class
Indinavir	−12.22	PI
Zidovudine	−9.39	NRTI
Amprenavir	−9.35	PI
Atazanavir	−8.98	PI
Saquinavir	−8.94	PI
Elvitegravir	−8.87	INSTI
Raltegravir	−8.50	INSTI
Nelfinavir	−8.33	PI
Abacavir	−8.08	NRTI
Lopinavir	−8.06	PI
Lamivudine	−7.63	NRTI
Delaviridine	−7.54	NNRTI
Tenofovir	−7.18	NRTI
Temsavir	−6.94	AI
Dolutegravir	−6.83	INSTI
Ritonavir	−6.64	PI
Nevirapine	−6.59	NNRTI
Darunavir	−6.39	PI
Doravirine	−6.24	NNRTI
Emtricitabine	−5.93	NRTI
Efavirenz	−5.48	NNRTI
Etravirine	−4.57	NNRTI
Rilpivirine	−4.56	NNRTI
Tipranavir	−4.51	PI
Maraviroc	−3.87	EI
Boceprevir	−9.04	PI for HCV, (positive control)
Oseltamivir	−7.75	Neuraminidase inhibitor, influenza (control)

Table 2.

Docking scores for HIV drugs tested against SARS-CoV-2 RdRp. The HIV ARV inhibitor class is also referenced (below).

Drug Name	Glide XP Score	Drug Class
Abacavir	−8.93	NRTI
Emtricitabine	−8.01	NRTI
Raltegravir	−7.81	INSTI
Zidovudine	−7.67	NRTI
Saquinavir	−7.51	PI
Lamivudine	−7.11	NRTI
Indinavir	−6.64	PI
Elvitegravir	−6.25	INSTI
Tenofovir	−6.12	NRTI
Nelfinavir	−6.03	PI
Dolutegravir	−5.93	INSTI
Rilpivrine	−5.52	NNRTI
Lopinavir	−4.86	PI
Atazanavir	−4.85	PI
Ritonavir	−4.68	PI
Doravirine	−4.67	NNRTI
Delavirdine	−4.54	NNRTI
Darunavir	−3.99	PI
Temsavir	−3.53	AI
Amprenavir	−3.50	PI
Etravirine	−2.99	NNRTI
Efavirenz	−2.89	NNRTI
Nevirapine	−1.61	NNRTI
Maraviroc	−0.13	EI
Tipranavir	ns	PI
GTP	−9.36	Control
ATP	−9.03	Control
Galidesivir	−8.52	RNA polymerase inhibitor

Drug Name	Glide XP Score	Drug Class
Remdesivir	−7.05	Nucleotide Analog

Table 3.

MM-GBSA results for the top Mpro-ligand hits calculated from MD trajectories of 250 ns.

Name	ΔG Average (kcal/mol)	ΔG Standard deviation
Amprenavir	−41.55	8.56
Atazanavir	−86.19	7.35
Indinavir	−51.44	6.62

Table 4.

MM-GBSA results for the top RdRp-ligand hits calculated from MD trajectories of 250 ns.

Name	ΔG Average (kcal/mol)	ΔG Standard deviation
Abacavir	−105.03	11.62
Emtricitabine	−102.24	10.67
Tenofovir	−96.71	13
Zidovudine	−93.49	9.47

Table 5.

Ongoing and planned clinical trials that use HIV antiretrovirals (ARVs) for the prevention and/or treatment of SARS-CoV-2. This table only includes trials that use HIV ARVs other than Lopinavir and Ritonavir.

Clinical Trial	Drugs being used in Trial for COVID-19
NCT04519125	**Tenofovir/ Emtricitabine (300 mg / 200 mg daily during 60 days)** + Personal Protective Equipment (PPE) vs. Placebo (1 tablet daily during 60 days) + PPE
NCT04359095	**Emtricitabine/tenofovir** vs. Colchicine + Rosuvastatin vs. **Emtricitabine/tenofovir** vs. Colchicine + Rosuvastatin vs. Standard treatment
NCT04441385	**Maraviroc 300 mg BID +** Standard care treatment vs Standard care
NCT04475991	**Maraviroc** + Currently used therapy|Procedure: Curently used therapy for COVID-19 non-critical patients| Favipiravir + Currently used therapy| **Maraviroc**+Favipiravir+CT
NCT04468087	**Atazanavir**| Daclatasvir 60 mg| Sofusbuvir + Daclastavir 60 mg| Placebo **Atazanavir**| Placebo Daclatasvir 60 mg| Placebo Sofusbuvir + Daclatasvir 60 mg| Daclatasvir 120 mg| Sofosbuvir + Daclatasvir 120 mg| Placebo Daclatasvir 120| Placebo Sofosbuvir/Daclatasvir 120
NCT04459286	Nitazoxanide and **atazanavir**/**ritonavir**| Standard of Care
NCT04405271	**Emtricitabine/Tenofovir Alafenamide 200 mg-25 mg Oral Tablet**| Placebo
NCT04435522	**Maraviroc**
NCT04261270	**ASC09F** *+Oseltamivir| **Ritonavir**+Oseltamivir| Oseltamivir
NCT04452565	NA-831|Combination Product: NA-831 and **Atazanavir**|Combination Product: NA-831and Dexamethasone|Combination Product: **Atazanavir** and Dexamethasone
NCT04425382	**Darunavir**/**Cobicistat**| **Lopinavir**/**Ritonavir**
NCT04334928	**Tenofovir Disoproxil Fumarat**e 245 mg/**Emtricitabine** 200 mg + Placebo of Hydroxychloroquine 200 mg vs. Hydroxychloroquine 200 mg + Placebo of Tenofovir Disoproxil Fumarate 245 mg/Emtricitabine 200 mg vs. **Tenofovir Disoproxil Fumarate** 245 mg/**Emtricitabine** 200 mg + Hydroxychloroquine 200 mg vs. Placebo
NCT04252274	**Darunavir** and **Cobicistat** (one tablet a day) vs. Conventional treatment
NCT04261907	**ASC09/ritonavir group**| **lopinavir/ritonavir group** **ASC09/ritonavir** (300mg /100mg) + conventional standardized treatment vs. **Lopinavir/ritonavir** (200mg / 50mg) + conventional standardized treatment

*__ASC09F__ is an investigational HIV protease inhibitor not yet approved by the FDA for use in the setting of HIV.

Table 6.

Clinical Trials and observational studies of PLWH or PrEP users, and the prevalence of COVID-19.

Clinical Trial	Title
NCT04575545	Prevalence of COVID-19 Infection in a Cohort of Patients Infected by the HIV and Patients Taking PrEP
NCT04581746	Impact of the Epidemic of COVID-19 Infection Among People Living With HIV (SARS-CoV-2)
NCT04333953	COVID-19 in Patients With HIV
NCT04361604	Clinical Characterisation Protocol for COVID-19 in People Living With HIV
NCT04357639	Impact of Long-term Protease Inhibitors in Patients Living With HIV on the Incidence of COVID-19 (COVIP)
NCT04526977	Differences in Immune Response Among HIV-1-infected Individuals With Previous or Current COVID-19 (CoVIHDis).
NCT04515225	COVID-19 Prevalence in HIV-infected Patients
NCT04523012	COVID-19 and HIV Patients
NCT04371835	COHIVE: Coronavirus (COVID-19) Outcomes in HIV Evaluation in Resource Limited Settings
NCT04379245	COVID-19 Infection in Patients Infected With HIV and/or on PrEP
NCT04514016	Cross Sectional CFAR HIV/COVID Study
NCT04533399	A Study Looking at the Effectiveness and Safety of a COVID-19 Vaccine in South African Adults
NCT04444674	COVID-19 Vaccine (ChAdOx1 nCoV-19) Trial in South African Adults With and Without HIV-infection
NCT04523090	Catalysing the Containment of COVID-19
NCT04354818	Coronavirus (COVID-19) Outcomes Registries in Immunocompromised Individuals Australia (CORIA)